

Comparing Current Flows in Ultrashallow pn-Schottky-like Diodes with 2-Diode Test Method

X. Liu, L.K. Nanver

Semiconductor Components, MESA+ Institute for Nanotechnology, University of Twente,
Enschede, the Netherlands

Abstract—A 2-diode test structure is proposed and investigated for use with simple $I-V$ measurements, giving an easy-to-process, fast turn-around-time method of comparing process-dependent current flows when developing ultrashallow/ Schottky junction technologies. Differential diode current characteristics and collector currents obtained from lateral transistor operation of the same 2-diode test structure are used to reliably identify the diode type and variations in metal-Si interfacial properties, independent of parasitic leakage currents. The versatility of this method with respect to diode geometry and substrate doping is verified for the measurement of junction- and Schottky-like diodes formed by different chemical-vapor-deposition processes.

Keywords—junction diodes, Schottky diodes, current-voltage characteristics, lateral bipolar transistor operation, chemical-vapor deposition, arsenic, phosphorus, boron

I. INTRODUCTION

In the development of semiconductor nanoscale devices, CMOS or alternatives, creating reliable atomically shallow diodes and ohmic contacts is of crucial importance [1]. Rather than applying impurity doping of the bulk semiconductor, interfaces can be structured to produce a source of charge carriers to create the desired junction behavior, an example of which is the PureB Si p^+n diode [2]. This diode, created by the interface reaction of a pure boron (B) layer deposited on Si, is used in the present investigation along with Schottky diodes made with arsenic (As) or phosphorus (P) chemical-vapor deposition [3]. With these devices a more thorough analysis is made of the 2-diode test structure first presented in [4] as a means of relating the diode $I-V$ characteristics to a gradual transition from Schottky-like to p-n junction-like behavior for diodes made with laser-annealing activation of surface dopants.

The 2-diode structure itself can be fabricated with a minimum of processing. Only the diodes and a contact to the substrate, n-type in this case, need to be processed. It is therefore well-suited for fast-turnaround-time process development. With only simple measurements it is possible to determine how significant the electron injection from the n-substrate into the p-Si/metal-contact region is with respect to the hole injection from this region into the substrate. In this paper, it is shown that the versatility of the method is considerably increased by considering the whole differential $I-V$ characteristic, particularly with respect to variations in the diode geometry and substrate doping. Examples are given demonstrating that the method not only gives

information on the diode type but also interfacial layers at the metal/Si interface resulting from variations in the junction processing can be identified. This method reduces the immediate need of more expensive and time-consuming temperature-dependent measurements or destructive material-analysis techniques.

II. EXPERIMENTAL PROCEDURES

All diodes were fabricated with or without a B, As or P pure dopant deposition at 700°C in contact windows to an n-type Si 2-5 Ω-cm 525-μm-thick substrate. In some cases an n^+ buried layer was fabricated under the diodes by burying a high-dose arsenic implantation under a 1-μm-thick epitaxially-grown lightly-doped n-type Si layer. The pure-dopant deposition conditions were chosen to give a complete coverage of the Si surface. An interconnect layer of Al/1%Si was sputtered directly after the deposition both on the front- and backside of the wafer that is the cathode terminal.

The pure B deposition has already been extensively studied and is known to form a few-nm deep p^+n -like junction with current flows comparable to a deep diffused junction [5]. Due to this likeness with respect to the $I-V$ characteristics, the PureB diodes studied here will in the following also be referred to as p^+n diodes. For the 700°C deposition used here, there is some boron doping of the Si surface to the solid solubility of $2 \times 10^{19} \text{ cm}^{-2}$. This is, however, not enough to explain the very low saturation current. Therefore, to explain this and other properties of these diodes, a new bandgap model was proposed in [6]. The deposited B layer provides a monolayer of acceptors at the interface which fill with electrons, giving a monolayer of fixed negative charge. The PureB layer acts like a semi-insulator accumulating an inversion layer of holes as illustrated in Fig. 1b.

In Fig. 1 also the band diagrams of conventional Schottky and ohmic-contacted p^+n junctions are shown with solid lines in Figs. 1a and 1c. In the ideal case with a lightly-doped n-substrate, the current in the p^+n diode is dominated by the injection of the holes from the p^+ -region into the n-substrate (Fig. 1a). In the Schottky diode, the current is dominated by the thermionic emission of electrons from the n-substrate into the metal (Fig. 1c, solid line). As a result, these two types of diodes can be discerned by identifying the type of the dominant current. The deposited As and P atoms are known to segregate as monolayers on the Si surface and it was shown in [3] that such layers can reduce

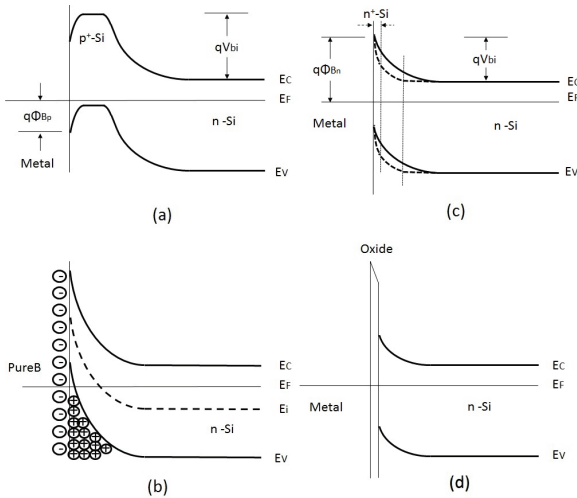


Fig. 1. Band diagram of a (a) conventional p+n diode, (b) PureB diode, (c) conventional Schottky diode (solid line) and Schottky diode with a highly-doped n⁺-region at the Si surface that is so narrow that the depletion still extends into the n'-region (dashed line) and (d) Schottky diode with a (tunneling) layer of oxide at the Si surface; all at zero bias.

the effective Schottky barrier height (SBH). It was proposed that this could be due to the passivation of acceptor-like states at the Si surface and/or a retarding of the formation of a native oxide on the Si before metallization. For the P deposition some doping of the bulk Si is also expected since the solid solubility is as high as $2 \times 10^{20} \text{ cm}^{-2}$ but the diffusivity is very low so only a few nm of the Si surface will be doped. Nevertheless, the very high doping would reduce the depletion width and give a very high electric field at the surface which would promote tunneling in addition to thermionic emission thus decreasing the effective SBH (Fig. 1c, dashed line). Without the P or As segregation, there may be some native oxide present before the metal sputtering as illustrated by the band diagram in (Fig. 1d).

III. TEST STRUCTURE DESIGN CONSIDERATIONS

The basic layout of a 2-diode test structure is shown in Fig. 2. The W_B is the distance between the emitter and collector and W_E is the emitter width. Schematic cross-sections of the diodes displaying the expected current flows are shown in Fig. 3 for the 3 biasing methods used here to study the emitter diode E.

To gain insight in the mechanisms governing the current flows in the different types of junction we first look at the ideal case, disregarding defect-induced currents. The electron and hole currents over a junction can be expressed as [7]:

$$I = qn_{i0}^2 A \left[\frac{1}{G_D} + \frac{1}{G_A} \right] \left(e^{\frac{qV}{kT}} - 1 \right) \quad (1)$$

$$I_h = \frac{qn_{i0}^2 A}{G_D} \left(e^{\frac{qV}{kT}} - 1 \right) \quad (2)$$

$$I_e = \frac{qn_{i0}^2 A}{G_A} \left(e^{\frac{qV}{kT}} - 1 \right) \quad (3)$$

where q is the elementary charge, n_{i0} is the intrinsic carrier concentration, A is the diode area, G_D and G_A are the Gummel numbers of the n- and p-doped regions, respectively, and kT/q is the thermal voltage. The electron injection into the anode (here the emitter/collector) region is governed by the Gummel number G_E of the region. In a general formulation this can be defined as

$$G_E = \int_{W_{QNE}} \frac{N_E(z)}{D_n(z)} \frac{n_{ie}^2(z)}{n_{ie}^2(z)} dz + \frac{N_E}{S_E} \frac{n_{ie}^2}{n_{ie}^2} \quad (4)$$

where W_{QNE} is the width of the p-type doped region of the Si, N_E is the active p-type doping concentration, i.e., hole concentration, $D_n(z)$ is the electron diffusion coefficient in the p-region as a function of depth z from the Si surface, and S_E is the surface recombination velocity. The $n_{ie}(z)$ is given by

$$n_{ie}(z) = n_{i0} \exp \left(\frac{-\Delta E_G(z)}{2kT} \right) \quad (5)$$

where $\Delta E_G(z)$ is the bandgap difference with respect to the c-Si. Likewise, the hole injection into the substrate is governed by the Gummel number of the substrate, G_{sub} . In the simplest 1-D approximation the saturation current can be written as $I_{SE} \propto 1/G_{sub}$ with $G_{sub} = N_{sub} W_{sub}$, where N_{sub} and W_{sub} are the substrate doping and width, respectively [7].

In all cases, for both p+n and Schottky junctions, the hole injection into the substrate will entirely be governed by the substrate doping profile if there is no bandgap difference at the junction to moderate it. Such a case is shown in Fig. 1d for the case of a thin native, possibly tunneling, oxide on the Si surface. Bandgap diagrams that plausibly describe this and the other junction situations described in this paper are collected in Fig. 1.

When the p⁺-region becomes so narrow that it approaches full depletion, the first component in (5) goes to zero and G_E becomes dominated by the surface recombination velocity at the metal contact. The resulting high electron injection dominates the current and becomes Schottky-like. In this type of junction the current is often described by an effective SBH, ϕ_B , with $I_{SE} \propto e^{-q\phi_B/kT}$.

A fundamental difference between the electron and hole current injection is found in the volume of the region into which they are injected. The emitter region is limited in size to the designed area of the contact windows, give or take some variations that may be caused by the actual processing. Therefore the injected electron current is proportional to the emitter area. In contrast, the holes injected into the substrate can spread in all directions into the substrate [8]. In our case with a low-doped 525-μm-thick substrate, the perimeter hole current per micrometer readily becomes much higher than the laterally uniform current density being vertically injected across the surface

area of the contact. The spreading of the holes will be attenuated by any hole injection from other diodes being operated in the vicinity. This effect is described in detail in [4] and is used here to extract information on the effect of junction processing on the current flows.

In some of the junctions studied here, a non-ideal current component is observed. The emitter current can be expressed as follows:

$$I_E = J_A A_E + J_P P_E + I_{\text{leak}} = I_{SE} \left(e^{\frac{qV}{kT}} - 1 \right) + I_{\text{leak}} \quad (6)$$

where A_E is the emitter area in which a laterally uniform current density J_A flows, P_E is the on-mask perimeter, J_P is the current per micrometer that then accounts for the current not included in $A_E J_A$, and I_{leak} is the non-ideal current component.

In Figs. 3c and 3d, only the emitter diode under investigation is connected and forward biased. In the p+n diode case, hole injection into the substrate dominates because electron injection into the emitter is suppressed by a high G_E . In the Schottky diode case electron injection dominates. In Fig. 3e and 3f, both the emitter and collector are connected and biased in forward and the current flow through the emitter is defined as $I_{E/C}$. The spreading of the holes injected from the emitter is limited by the holes spreading from the collector, making $I_E > I_{E/C}$. For the p+n case, dominated by hole injection, $\Delta I_E/I_E$, with $\Delta I_E = I_E - I_{E/C}$, will be large but for the Schottky case, dominated by high electron injection, it is expected to be low.

In Fig. 3a and 3b, the emitter and collector are biased as a lateral bipolar transistor in forward active mode with the substrate as base so $I_E = I_B + I_C$. The I_C is governed by the effective base Gummel number, G_B , that for ideal pn- and metal-Si junctions is determined by the distance and integral doping between the E and C contacts. For the Schottky case, any interfacial (semi-)isolating layers can also contribute to suppressing both the hole injection and the electron injection from the substrate.

IV. RESULTS AND DISCUSSION

The $I-V$ characteristics of an As-deposited Schottky diode and a p+n diode with $N_{\text{sub}} = 10^{15} \text{ cm}^{-3}$ are shown in Fig. 4, along with the extracted ΔI_E . The visible differences between I_E and $I_{E/C}$ are typical for the two types of diodes: for the p+n diode, the relative current discrepancy, $\Delta I_E/I_E$, is large in the low current ideally exponential region because the spreading of the hole current is restricted by the current flow from the adjacent diode. As the current increases with voltage, the discrepancy becomes small relative to the I_E because the current increase becomes attenuated by series resistance. The opposite is true for the Schottky case because ideally the electron current is proportional to the diode area, unaffected by the spreading through the substrate. This spreading is, however, restricted when the collector is contacted and this increases the effective series resistance through the substrate. This is seen as an

increasingly large discrepancy when high current levels are reached.

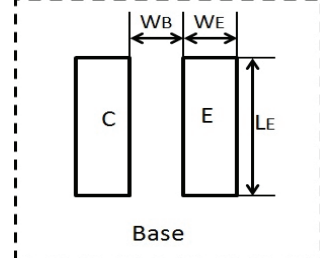


Fig. 2. Basic layout of the 2-diode test structure.

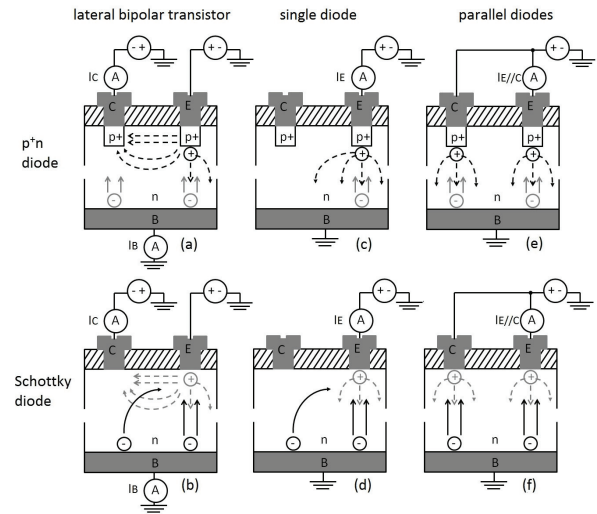


Fig. 3. Schematic cross-section of the 2-diode test structure for 3 different biasing methods. The expected current flows are indicated by black arrows for the dominant carrier flows and light grey arrows the other carrier-type flows. The hole flows are represented by dashed lines and the electron flow by solid lines. The top row is for p+n-like diodes and the bottom row for Schottky-like diodes.

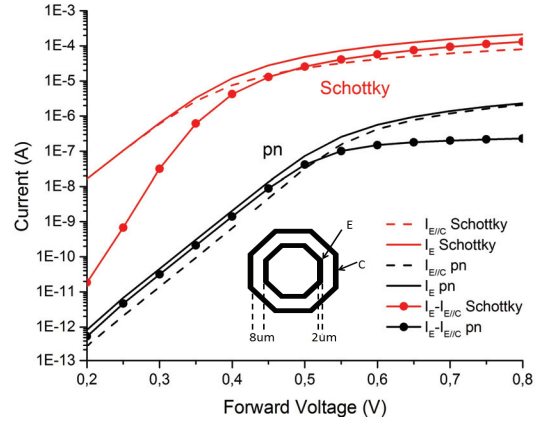


Fig. 4. I_E , $I_{E/C}$ and ΔI_E as a function of forward voltage for Schottky diode (in red) and a PureB diode (in black). The substrate doping is 10^{15} cm^{-3} . The schematic gives the dimensions of the measured 2-diode structure; the emitter is 431 μm long.

A. Substrate Doping Concentration

In Fig. 5 the hole diffusion length L_p and lifetime are shown as a function of n-doping of the substrate [9-10]. For p⁺n diodes, the hole spreading into the substrate is determined by the L_p [8] and is reduced when increasing the n-doping level. Therefore, the $\Delta I_E/I_E$ is expected to be larger for low doping levels. Examples of this will be given in the following sub-section along with a discussion of the influence of leakage currents.

B. Leakage currents

In Fig. 6 the $I-V$ characteristics are shown for test structures with and without an n⁺-layer buried. This layer increases the G_{sub} , which is seen as a significant decrease in the levels of I_E and $I_{E/C}$. However, below 0.4 V, the curves are dominated by a non-ideal current component and all the currents appear to fall on top of each other. Nevertheless, the ΔI_E is not significantly affected by either the buried layer or the leakage current. The former is understandable because the buried layer is only present in the top couple of micrometer of the substrate and cannot affect the overall hole spreading very much. Moreover, despite the leakage current, the ΔI_E displays an ideality factor of $n \sim 1$ over the whole low voltage region before the series resistance attenuates I_E . This can be explained by considering that, in view of the limited processing, it is to be expected that the leakage component originates from defects in or near the depletion region over the emitter junction and not in the bulk of the substrate into which the hole current spreads. This leakage is therefore the same whether or not the collector is connected. By using an emitter area, A_E , that covers a laterally uniform current-flow region in both contacting situations, we can write:

$$I_E = J_E A_E + J_{PE} P_E + I_{\text{leak}} = I_{SE} \left(e^{\frac{qV}{kT}} - 1 \right) + I_{\text{leak}} \quad (7)$$

$$I_{E||C} = J_E A_E + J_{PE||C} P_E + I_{\text{leak}} = I_{SE||C} \left(e^{\frac{qV}{kT}} - 1 \right) + I_{\text{leak}} \quad (8)$$

Therefore $\Delta I_E = I_E - I_{E||C}$ follows the ideal $I-V$ characteristic

$$\Delta I_E = J_{PE} P - J_{PE||C} P = (I_{SE} - I_{SE||C}) \left(e^{\frac{qV}{kT}} - 1 \right) \quad (9)$$

This validates that plotting the whole $\Delta I_E(V)$ curve is a very sensitive means of monitoring the hole injection. In contrast, as listed in Table I, the relative discrepancy $\Delta I_E/I_E$ remains below 1% for voltages below 0.4 V and only becomes a peak value of 45% at 0.6 V after which the series resistance inhibits further increase.

Table I also includes $\Delta I_E/I_E$ for 3 p⁺n test structures with an N_{sub} of either 10^{15} , 10^{17} or 10^{18} cm^{-3} . In this case the G_{sub} increases accordingly, thus decreasing the ideal but also the non-ideal current component as can be seen in Fig. 7a. Both effects reduce the sensitivity of $\Delta I_E/I_E$ which is only a few percent when leakage dominates. The $\Delta I_E(V)$ curves are nevertheless near-ideal, even for $N_{\text{sub}} = 10^{18} \text{ cm}^{-3}$ for which the spreading current level is very low and I_E is totally dominated by the leakage current. In Fig. 7b, the corresponding Gummel plots are shown. The I_C decreases by decades as the doping, and thus G_B , increases. Leakage

currents are visible in the I_B curves: for the lightest substrate doping emitter-base leakage increases the low-voltage I_B while collector-base leakage is visible below 0.35 V for the two higher substrate doping levels. Nevertheless, the ideality factor n is approximately 1 in all cases and is also not affected by leakage currents.

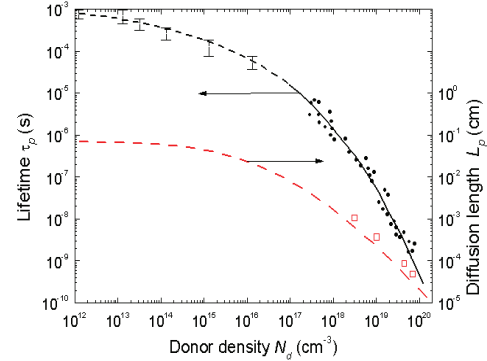


Fig. 5. Hole diffusion length and lifetime as a function of n-doping of the substrate [9-10].

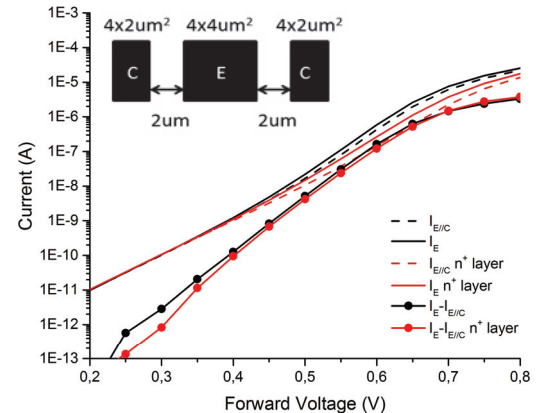


Fig. 6. I_E , $I_{E/C}$ and ΔI_E as a function of forward voltage for PureB diodes with (in red) and without (in black) an n⁺ buried layer. The $N_{\text{sub}} = 10^{15} \text{ cm}^{-3}$. The schematic gives the dimensions of the measured 2-diode structure.

TABLE I. RELATIVE CURRENT DISCREPANCY FOR THE PUREB DIODES MEASURED IN FIGS. 6 AND 7, WITH VARIOUS SUBSTRATE DOPING LEVELS

Forward Voltage [V]	$\Delta I_E/I_E [\%]$ for given N_{sub}			Dominating Effect	
	Buried n ⁺ -layer				
	10^{15} cm^{-3}	10^{17} cm^{-3}	10^{18} cm^{-3}		
0.2	0.3%	0.1%	14.3%	leakage current	
0.3	0.7%	2.7%	17.5%	leakage current	
0.4	0.8%	10.3%	16.9%	ideal diode	
0.5	28.5%	23.8%	16.1%	ideal diode	
0.6	45.8%	27.8%	9.9%	ideal diode	
0.7	40.0%	19.3%	3.7%	series resistance	
0.8	21.5%	13.0%	2.0%	series resistance	

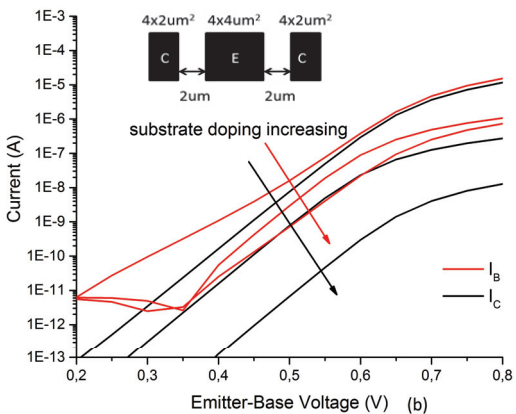
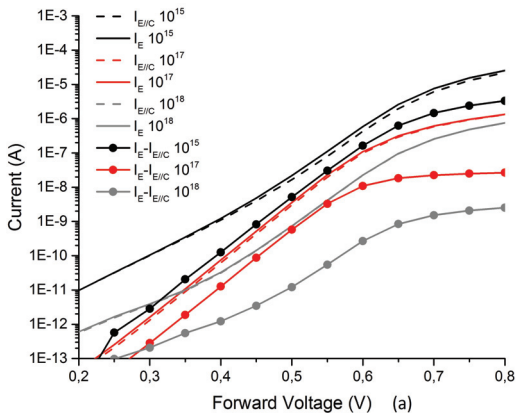


Fig. 7: Measurements of PureB diodes with an N_{sub} of either 10^{15} , 10^{17} or 10^{18} cm^{-3} . (a) I_E , I_E/C and ΔI_E as a function of forward voltage, and (b) Gummel plots. The schematic gives the dimensions of the measured 2-diode structure.

TABLE II. RELATIVE CURRENT DISCREPENCY FOR PUREB DIODES WITH DIFFERENT E-C DISTANCES AND GEOMETRIES

Forward Voltage [V]	$\Delta I_E/I_E [\%]$ for Different E-C Distances			Dominating Effect
	$2 \mu\text{m}^a$	$65 \mu\text{m}^b$	$80 \mu\text{m}^c$	
0.2	1.8%	1.7%	1.0%	leakage current
0.3	3.9%	2.7%	1.1%	leakage current
0.4	20.7%	3.1%	1.1%	ideal diode
0.5	52.9%	3.6%	1.2%	ideal diode
0.6	70.0%	7.1%	2.3%	ideal diode
0.7	55.0%	21.2%	7.8%	series resistance
0.8	36.3%	32.3%	12.5%	series resistance

a: on-mask emitter area $4 \times 4 \mu\text{m}^2$, collector area $4 \times 2 \mu\text{m}^2$

b: on-mask emitter area $20 \times 20 \mu\text{m}^2$, collector area $50 \times 50 \mu\text{m}^2$

c: on-mask emitter area $20 \times 20 \mu\text{m}^2$, collector area $20 \times 20 \mu\text{m}^2$

C. Test Structure Geometry

Obviously, the ΔI_E will be highest if the emitter and collector diode are as close as possible to each other. The limits to this are set by the design rules or the design that happens to be available. The doping of the substrate also

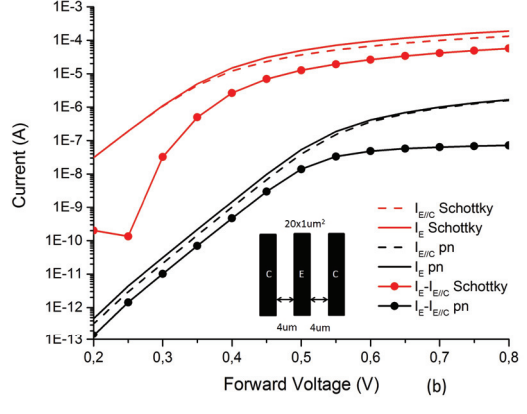
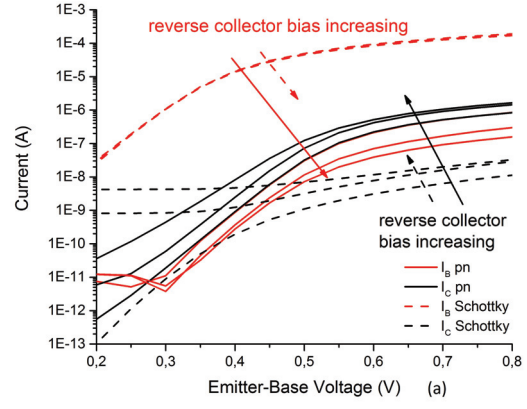


Fig. 8: (a) Gummel plots for As-deposited-Schottky and PureB diodes. I_B is in red and I_c in black. The reverse bias is stepped as 0, 0.5 V and 1 V. (b) The I_E , I_E/C and ΔI_E as a function of forward voltage. The substrate doping is 10^{15} cm^{-3} and the schematic gives the dimensions of the measured 2-diode structure.

sets a limit because for W_B in the range of the depletion widths, reach-through may occur. In that case the measurement of the I_c could drown in a punch-through current, an example of which is shown in the Gummel plot of Fig. 8a. However, as can be seen for the diode $I-V$ characteristics shown in Fig. 8b, the ΔI_E is not effected by punch-through.

Measurements on a wafer with $N_{\text{sub}} = 10^{15} \text{ cm}^{-3}$ with structures with different W_B and diode sizes are shown in Fig. 9. In Table II a number of results are also listed for the corresponding $\Delta I_E/I_E$ values. As the distance gets larger the discrepancy loses sensitivity with values around 1% for the largest distances. The current level of ΔI_E curve decreases in value but still is a clear witness of the hole injection.

D. Interfacial Layers

Gummel plots for test structures with and without a surface deposition of either B, As, or P are shown in Fig. 10. The diode area is $20 \times 1 \mu\text{m}^2$ and $W_B = 3.5 \mu\text{m}$. The I_B is highest for the P deposition, presumably because the surface doping with P, which is possible to about $2 \times 10^{20} \text{ cm}^{-3}$,

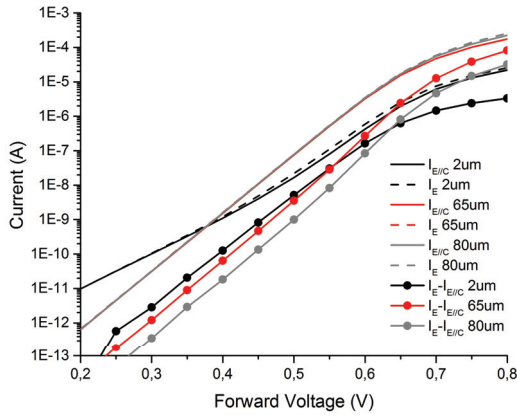


Fig. 9: Measurements of test structures with the different geometries given in Table II. I_E , $I_{E/C}$ and ΔI_E as a function of forward voltage for PureB. The $N_{\text{sub}} = 10^{15} \text{ cm}^{-3}$.

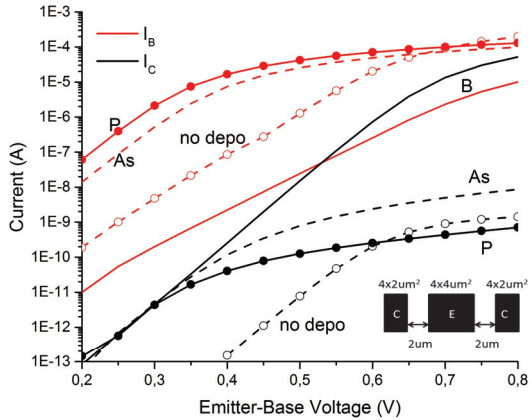


Fig. 10: Gummel plots for test structures without and with a surface deposition of either B, As or P. I_B is in red and I_C in black. The substrate doping is 10^{15} cm^{-3} . The schematic gives the dimensions of the measured 2-diode structure.

lowers the Schottky barrier height. For the structure without a deposition to protect the Si surface against native-oxide formation the I_B is 2 decades lower and non-ideal, indicating that oxide is present at the interface and increases the effective G_E . In contrast to the other structures, the I_C in this case deviates from the low forward-voltage current level of the p⁺n I_C curve. This suggests that the effective G_B is increased by the presence of oxide at the interface, i.e., there is no longer a “clean” metal-Si interface.

In contrast to the p⁺n junctions, the ΔI_E of the Schottky-like diodes display an $n < 1$ that decreases as the I_E (electron current) decreases and the attenuation from series resistance decreases. When I_E becomes so low that the series resistance no longer influences it, the ΔI_E would become a result of the hole current spreading. However, the I_E of the two Schottky diodes used here is too high for the ΔI_E to become so low that only the result of hole spreading is visible.

V. CONCLUSIONS

The 2-diode test structure gives an easy-to-process, fast-turn-around-time method of comparing the carrier flows responsible for the $I-V$ characteristics of ultrashallow/Schottky junctions. The present results show that the slope of the $\Delta I_E - V_{BE}$ characteristics for pn-like junctions remains near-ideal in spite of large parasitic leakage-current components in I_E and/or poor device geometry and can therefore much more reliably identify pn behavior than the relative current change $\Delta I_E/I_E$. For Schottky-like diodes not only the I_E but also the I_C can reveal changes in the metal-Si interfacial properties that may modify both the effective emitter and base Gummel number.

REFERENCES

- [1] R. T. Tung, “The physics and chemistry of the Schottky barrier height,” *Applied Physics Reviews*, vol. 1, pp. 011304(1-54), 2014.
- [2] L. K. Nanver, L. Qi, et al., “Robust UV/VUV/EUV PureB photodiode detector technology with high CMOS compatibility,” *J. Select. Topics Quantum Electronics*, vol. 20, no.6, pp. 1_11, Nov. 2014.
- [3] Q. W. Ren, W. D. van Noort, L. K. Nanver and J. W. Slotboom, “Metal/silicon Schottky barrier lowering by RTCVD interface passivation,” *Proc. ECS*, 2000(9), pp. 161-166, 2000.
- [4] L. Qi, G. Lorito, L. K. Nanver, “Lateral-transistor test structure for evaluating the effectiveness of surface doping techniques” *IEEE Trans. Semiconductor Manufacturing*, vol. 25, no. 4, pp. 581-588, Nov. 2012.
- [5] F. Sarubbi, L. K. Nanver and T. L. M. Scholtes, “High effective Gummel number of CVD boron layers in ultrashallow p⁺n diode configurations,” *IEEE Trans. Electron Devices*, vol. 57, no. 6, pp. 1269-1278, Jun. 2010.
- [6] L. Qi, and L. K. Nanver, “Conductance along the interface formed by 400 °C pure boron deposition on silicon,” *IEEE Electron Device Letters*, vol. 36, no.2, pp. 102-104, Dec. 2014.
- [7] S. M. Sze and K. K. Ng, *Physics of Semiconductor Devices*, 3rd edition, John Wiley & Sons, Inc., USA, 2007.
- [8] P.-J. Chen, K. Misiakos, A. Neugroschel, and F. A. Lindholm, “Analytical solution for two-dimentional current injection from shallow p-n junctions,” *IEEE Trans. Electron Devices*, vol. 32, no. 11, pp. 2292-2296, Nov. 1985.
- [9] Alamo, J.A., and R. M. Swanson, “Modeling of minority carrier transport in heavily doped silicon emitters”, *Solid-State Electronics* vol. 30, no. 11, pp. 1127-1136, Nov. 1987.
- [10] <http://www.ioffe.rssi.ru/SVA/NSM/Semicond/Si/electric.html>